International Journal of Engineering Sciences Paradigms and Researches (IJESPR)
Volume 46, Issue: Special Issue of December 2017
An Indexed, Referred and Peer Reviewed Journal with ISSN (Online): 2319-6564
www.ijesonline.com

Using time domain and geographic source tracers to conceptualize streamflow generation processes in lumped rainfall-runoff models

[1] Prativa Samal, [2]Sradhananda Ghadei*
[1] Assistant Professor, Dept. Of Civil Engineering, NIT BBSR,*
[2]Asst. Professor DEPT. of Civil Engineering, HIT, BBSR
[1] prativasamal@thenalanda.com, sradhanandaghadei123@gmail.com*

Abstract:

Using isotopes and geochemical tracers obtained from a field investigation in a 3.6 km2 highland catchment in Scotland, the temporal dynamics and geographical sources of streamflow were modelled in a lumped rainfall-runoff model (isoSAMdyn). A hydrological year's worth of high-resolution (daily) stable isotope measurement of precipitation and streamflow, along with fortnightly groundwater and riparian saturation zone sampling, permitted the testing of runoff formation process theories. They were modelled in a previously created model (SAMdyn) based exclusively on geochemically defined geographic source tracers, which demonstrated that the primary mechanism for storm runoff generation in the catchment is the nonlinear dynamic expansion and contraction of riparian saturation regions. SAMdyn produced a good simulation of streamflows and alkalinity (as a source tracer), but it was unable to replicate the dynamics of deuterium's rainfall-runoff (62H). Improved 62H simulations in stream water and the main catchment water stores were achieved by using the model in a learning framework, incorporating parameters for passive storage in catchment hillslopes and groundwater mixing in riparian saturation zones, along with associated isotopic fractionation. The resulting conception of rainfall-runoff processes brought together hydrometric data, geochemical signals, and isotopic signals in a significant way. The fractionation of water in surface saturation zones in this specific catchment, however, seems to be a complicated process that prohibits the simulation of short-term isotope dynamics in the stream during the summer.

1. Introduction

[1] Conceptualization of streamflow generation processes and integration into rainfall-runoff models remains a major research challenge in catchment hydrology [*Lischeid*, 2008 ; *Tetzlaff et al.*, 2008a]. Despite more than a decade of closer collaboration between field experimentalists and modelers [e.g., *Seibert and McDonnell*, 2002], there remains much debate over what is the appropriate level of model parameterization and how best to ensure that models give the right answers for the right reasons [*Kirchner*, 2006]. Recently, the integration of field-derived tracer data in rainfall-runoff models has been shown to be a potentially useful research tool in this regard [e.g., *Uhlenbrook and Leibundgut*, 2002 ; *Dunn et al.*, 2003]. Geochemical tracers provide insights into the geographical sources of streamflow [e.g., *Hooper*, 2001] and isotopic (or other conservative) tracers into the temporal dynamics of runoff processes [e.g., *Pearce et al.*, 1986]. However, it is not uncommon that hydrometric, geochemical, and isotopic signals provide apparently contradictory insights into catchment function [*Kirchner*, 2003] which can be difficult to reconcile in terms of understanding and modeling the hydrological response [*McDonnell et al.*, 2007].

[2] Until relatively recently, logistical and financial constraints often resulted in marked differences in the temporal resolution of hydrometric data (typically 15 min) and isotopic tracer data (often weekly) [*Kirchner et al.*, 2004]. Improvements in the reliability of automatic water samplers and, more importantly, the recent availability of laser spectroscopy facilitate high-resolution daily or subdaily sampling over long periods at relatively low cost [e.g., *Lyon et al.*, 2009; *Birkel et al.*, 2010b]. This provides a rich resource for incorporating field-based insights in hydrological models, which may have previously been masked by coarse sampling time steps [*Berman et al.*, 2009].

[3] While both geochemical tracers and stable isotopes have been used to constrain and evaluate rainfall-runoff models [e.g., *De Grosbois et al.*, 1988; *McGuire et al.*, 2006; *Fenicia et al.*, 2008], they have rarely been used simultaneously. Yet such dual-tracer approaches have powerful potential in hypothesizing both the sources of runoff and their temporal dynamics [e.g., *Katsuyama et al.*, 2009] and testing these hypotheses within a modeling-based learning framework [*Vache´ and McDonnell*, 2006; *Beven*, 2007; *Dunn et al.*, 2008]. This approach also has the possibility of exploring the nature of storage-discharge relationships, which are usually parameterized within rainfall-runoff

models but may provide fundamental insights into catchment function [e.g., *Kirchner*, 2009]. For example, isotope studies have shown that the total catchment storage is likely to be much greater than the dynamic storage inferred by hydrometric data alone [e.g., *Soulsby et al.*, 2009], which needs to be invoked to explain nonlinearity in rainfall-runoff responses in relation to antecedent conditions [e.g., *Dunn et al.*, 2010]. This larger, more passive (often called immobile) water storage has long been cited as an explanation for the observed damping of streamflow isotope signatures compared to precipitation [*Barnes and Bonell*, 1996] and the long tailing of residence time distributions [*Kirchner et al.*, 2000] by retaining water for long periods before release [*Spence*, 2007]. A better understanding of the spatial distribution of water stores and temporal dynamics of water release mechanisms in catchments is therefore needed to enhance the conceptualization of catchment functioning in rainfall-runoff models [*Soulsby et al.*, 2008]. Again, dual-tracer applications in conceptual hydrological models have utility if tracer data from different hydrological stores can help to internally verify a model and the applied storage conceptualization [*Seibert and McDonnell*, 2002; *Tetzlaff et al.*, 2008b].

[4] In different geographical regions, the relationships between landscape organization and catchment hydrological response vary as the dominant runoff generation processes change [e.g., *Tetzlaff et al.*, 2009a]. Differences in topography, soil cover, and climate interact to govern the catchment hydrological response [*Hrachowitz et al.*, 2009]. In glaciated landscapes such as the Scottish Highlands, the catchment soil cover reflects the interactions between climate, topography, parent material, and land use. Soil hydrological characteristics play a key role in controlling catchment rainfall-runoff responses [*Soulsby et al.*, 2006]. Previous field and modeling studies in such environments have shown the importance of dynamically expanding and contracting riparian saturation zones, often related to organic-rich peaty (histic) soils which have developed on poorly drained drift deposits [*Seibert et al.*, 2003 ; *Birkel et al.*, 2010a]. Riparian saturation zone dynamics reflect catchment connectivity and control the generation of quick, near-surface runoff processes [*Tetzlaff et al.*, 2007a]. As such, runoff mechanisms are dependent on the linkages between the saturated areas and their surrounding hillslopes, and the hydrological response is highly nonlinear in relation to antecedent conditions [*Tetzlaff et al.*, 2008a]. Therefore, understanding the role of the riparian zone on nonlinear runoff generation and mixing of waters originating from different sources is crucial to modeling water and solute transport [*Seibert et al.*, 2009].

[5] Here we extend earlier work in the Girnock, a Scottish upland catchment, which used field-based process insights to develop a tracer-aided rainfall-runoff model (SAM^{dyn}) to simulate flow and geographical source area tracer responses on the basis of nonlinear saturated area dynamics [*Birkel et al.*, 2010a]. The present study sought to incorporate high-resolution time domain tracers (stable isotopes) as a further means of model evaluation in terms of the temporal dynamics of rainfall-runoff processes. The study combined field and modeling components with the following objectives: First, to characterize the isotopic and geochemical signature of the major water stores and fluxes

of the catchment hydrological system over a hydrological year. Here particular attention was focused on the acquisi- tion of high-resolution (daily) isotope analysis of precipita- tion and streamflow to understand the temporal dynamics of rainfall-runoff processes. Second, using these data tounderpin the evolution of the original SAM^{dyn} model to be able to simulate the temporal dynamics of both time do- main and geographic source tracers in major catchmentstores and fluxes within an internally consistent conceptual rainfall-runoff model (isoSAM^{dyn}). Finally, we seek to out- line the challenges and limitations of such a dual-tracer approach in conceptual modeling.

2. Study Site

[6] The Bruntland Burn (BB) is a subcatchment of the Girnock Burn experimental catchment, which drains into the River Dee and is located in the Cairngorms National Park, Scotland (Figure 1). Full details of the Girnock catch- ment are given by *Tetzlaff et al.* [2007a] and *Soulsby et al.* [2007]. The BB subcatchment drains 3.6 km^2 with a mean altitude of 350 m above sea level (asl). Annual precipitation, mainly from westerly frontal systems, is around 1000 mm, with the summer months (May– July) generally being driest [*Tetzlaff et al.*, 2005]. Annual runoff is about 600 mm. The landscape has been glaciated and has typical landforms such as steep slopes and wide valley bottoms. Land cover is dominated by heather (*Calluna vulgaris*) moorland (20%), peat bogs (13%), and an area of commercial forestry (34%) on the steeper hillslopes near the catchment outlet. The east-ern hillslopes are underlain by granite, which occupies 46% of the catchment. The bedrock on the western and southern flanks (45% of the catchment) is dominated by schists and other metamorphic rocks (9%) [*Soulsby et al.*, 2007]. Frac- tured bedrock outcrops occupy 29% of the catchment area, particularly at high elevation, and are likely to be important recharge zones [*Tetzlaff et al.*, 2007b].

[7] Much of the catchment's lower slopes are covered by glacial drift deposits, particularly low-permeability till in the valley bottoms, upon which hydrologically responsive gley and peat soils (covering about 61% of the area) have formed. These roughly map on to the area of maximum sat- uration (Figure 1) and are well connected to the stream channel network [*Tetzlaff et al.*, 2009b]. Process studies have shown that such soils are near saturation for much of the year and the saturated areas dynamically expand and contract according to wetness conditions ranging between 2% and 40% of the total area [*Birkel et al.*, 2010a]. These saturation areas generate substantial amounts of saturation excess overland flow and shallow lateral flow in organic surface horizons. The second most common soil unit (39% of the catchment) comprises freely draining brown earths (cambic) on steeper hillslopes which generally remain un- saturated. Vertical water movement mainly facilitates groundwater recharge in such soils [*Soulsby et al.*, 1998]. *Soulsby et al.* [2005] have indicated that a portion of groundwater recharge probably moves quickly through shallow fracture systems [e.g., *Shand et al.*, 2006] or freely draining drift deposits to discharge into valley bottom areas. This discharge emerges either as hillslope seepage return flow into the area of saturated peaty soils or through the bed and banks of the stream [*Malcolm et al.*, 2006].

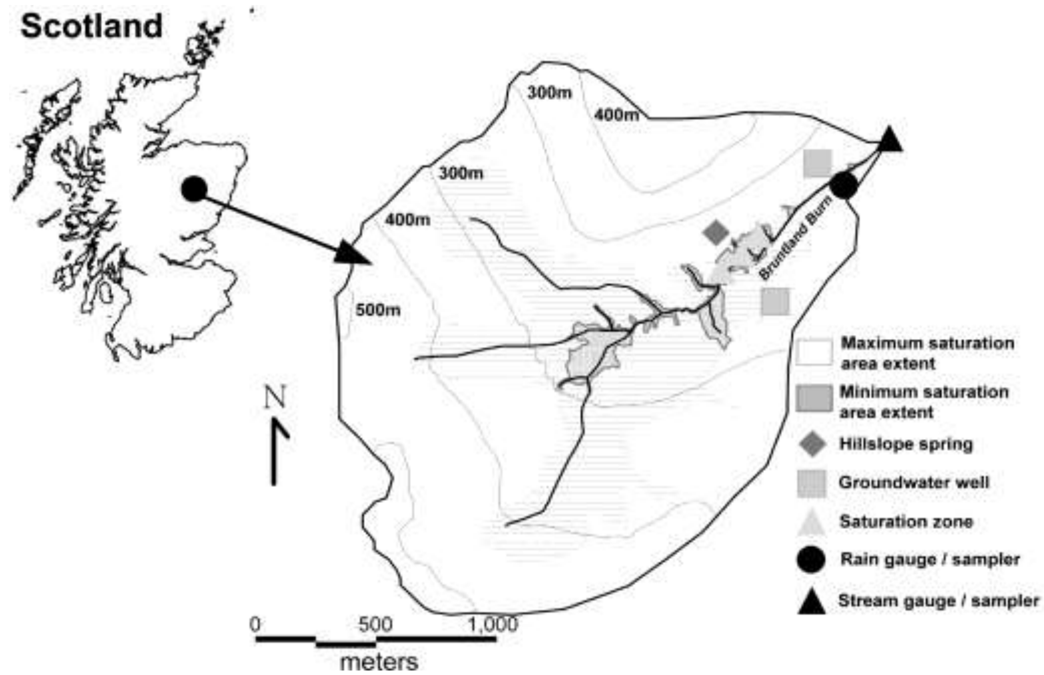

Figure 1. Bruntland Burn catchment topography, sampling locations, and mapped maximum and minimum saturation area extent (Stream gauge grid reference: NO 324956).

3. Data Sources

Hydrology

[8] Discharge (15 min resolution) was measured in a natural rated section (Figure 1) using an Odyssey capacitance rod. Rainfall (15 min resolution) was recorded by a tipping bucket gauge (HOBO) sited at an altitude of 300 m asl near the catchment outlet (Figure 1). Actual evapotranspiration (ET) was estimated by a Penman-Monteith equation adjusted to aerodynamic and canopy roughness characteristics of the study site [*Dunn and Mackay*, 1995]. Meteorological data were used from stations located ∼20 km from the catchment (operated by the Macaulay Land Use Research Institute) and located ∼3 km from the catchment (operated by Marine Scotland).

Stable Isotopes

[9] Daily precipitation and stream isotope sampling was undertaken using ISCO 3700 automatic water samplers from 1 September 2008 through 6 October 2009 (Figure 1). Stream samples were taken instantaneously at 8 :00 A.M., and precipitation samples were taken at the same time but represented accumulations over the preceding 24 h (Table 1). During the winter (December – February), only weekly stream samples were possible because of a malfunction of the automatic sampler during frosts. Paraffin oil was applied to the sample bottles to avoid evaporation losses [*International Atomic Energy Agency*, 2009]. The deuterium ($^{2}H/^{1}H$) and oxygen-18 ($^{18}O/^{16}O$) ratios were simultaneously determined with a Los Gatos Research DLT–100 laser diode water isotope analyzer using a standard analytical protocol [*Lis et al.*, 2008 ; *Birkel et al.*, 2010b]. Data were transformed into the 6 notion (6^{2}H and 6^{18}O in %) according to Vienna standard mean ocean water (VSMOW) standards. We analyzed both 6^{2}H and 6^{18}O, but because of

International Journal of Engineering Sciences Paradigms and Researches (IJESPR)
Volume 46, Issue: Special Issue of December 2017
An Indexed, Referred and Peer Reviewed Journal with ISSN (Online): 2319-6564
www.ijesonline.com

the interdependence of both isotopes, greater precision, and variability over wider range, we only consider 6^2H for the model simulations. Average precision for the instrument was 0.63% and 0.25% for 6^2H and 6^{18}O, respectively.

[10] In addition, fortnightly groundwater samples were taken at two deep wells and from a spring at a lower hill-slope seepage (Figure 1). Overland flow waters were sampled at three different locations of perennial saturation, again on a fortnightly basis, but starting slightly later on 1 January 2009 (Table 1). Snow samples were taken and ana- lyzed for stable isotopes during a 2 week period of snow in the catchment at the end of February 2009.

Geochemistry

[11] We also analyzed stream, groundwater, and saturated area samples for alkalinity on a weekly or fortnightly basis. Unfortunately, daily stream samples could not be used because of potential contamination by the paraffin. Alkalinity (in μeq L^{-1}) is a measure of the acid-neutralizing capacity of waters and was determined by acidimetric titration (0.005 M H_2SO_4) to the end point pHs 4.5, 4, and 3 using an Eppendorf pipette with a precision of 61% [*Neal et al.*, 1997]. It essentially reflects the geographic sources of water: In many Scottish upland catchments, low flows are dominated by high alkalinities, showing a clear geologi- cal imprint of groundwater, while storm runoff is derived from acidic, upper soil horizons with alkalinities close to zero [*Soulsby et al.*, 2007]. The close relationship between measured stream alkalinity concentrations and discharge (2003 – 2008, $R^2 > 0.8$) has been demonstrated for the Gir- nock by *Tetzlaff et al.* [2008b]. This has been used as a ba- sis for parameterizing alkalinity in groundwater and soil water sources in the SAM^{dyn} model, as described by *Birkel et al.* [2010a].

International Journal of Engineering Sciences Paradigms and Researches (IJESPR)
Volume 46, Issue: Special Issue of December 2017
An Indexed, Referred and Peer Reviewed Journal with ISSN (Online): 2319-6564
www.ijesonline.com

Table 1. Sampling Resolution and Collection Method

	Component	Resolution	Method
Hydrology	Precipitation	15 min	Tipping bucket
	Discharge	15 min	Rating curve
	Actual ET	Hourly	Penman-Monteith
Geochemistry	Stream alkalinity	Weekly	Spot
	Saturation zone alkalinity	Sporadic	One location
	Groundwater alkalinity	Sporadic	One location
Isotopes	Precipitation δ^2H	Daily	Accumulated
	Snow δ^2H	Sporadic	Spot
	Stream δ^2H	Daily (8:00 A.M.)	Spot
	Groundwater δ^2H	Fortnightly	Two locations
	Hillslope spring δ^2H	Fortnightly	One location
	Saturation zone δ^2H	Fortnightly	Three locations

4. Model Development

[13] A daily rainfall-runoff model, the dynamic saturation area model (SAM^{dyn}), has been developed for the Girnock catchment and is fully described by *Birkel et al.* [2010a]. Briefly, the model is a lumped, conceptual, tracer-aided water balance model that simulates daily runoff. The model is driven by daily precipitation inputs (P_{up}, P_{sat}) equivalent to the difference of precipitation rate and actual evapotranspiration rate into a conceptualization that dynamically links hillslope, saturation area, and groundwater reservoirs (Figure 2a). The dynamic structure of the model uses an empirically based time series of an estimated saturation zone extent (dyn_fSAT) calibrated against the GPS-mapped saturated catchment area to dynamically vary the storage volumes according to the wetness condition, where a greater wetness results in a smaller hillslope storage area (A_{up}) and expanded saturation areas (A_{sat}). A 7 day antecedent precipitation exponential decay function was found to best represent the wetness conditions and resulting saturation zone extent in the Girnock catchment.

[14] A water balance is calculated at each time step for the hillslope S_{up}, groundwater S_l, and saturation area storage S_{sat} of the SAM^{dyn} model:

$$S_{up(t)} = S_{up(t-1)} + \left[\left(P_{up(t)} - ET_{up(t-1)}\right)A_{up} - R_{(t-1)} - Q_{up_{(t-1)}} \right] \Delta t; \quad (1)$$

$$S_{l(t)} = S_{l_{(t-1)}} + \left(R_{(t)} - Q_{l(t-1)}\right)\Delta t; \quad (2)$$

$$S_{sat(t)} = S_{sat_{(t-1)}} + \left[Q_{up(t)} - Q_{sat(t-1)} + \left(P_{sat_{(t)}} - ET_{sat(t-1)}\right)A_{sat} \right] \Delta t; \quad (3)$$

where R (m^{3}s^{-1}) is recharge to the lower storage S_l (m^3); P_{up} and P_{sat} (m s^{-1}) are precipitation input into the total hillslope storage S_{up} (m^3) and saturation area storage S_{sat}, respectively; ET is actual evapotranspiration (m s^{-1}); and the dynamic A_{up} and A_{sat} are in m^2. Total discharge Q (m^{3}s^{-1}) is the sum of the discharge from both the saturation area storage Q_{sat} and lower groundwater storage Q_l. Dis- charge from the hillslope Q_{up} (m^{3}s^{-1}) is routed into the sat- uration area storage S_{sat} (Figure 2a).

[15] The following equations define the linear storage-discharge fluxes from the upper (S_{up}) and lower storage (S_l):

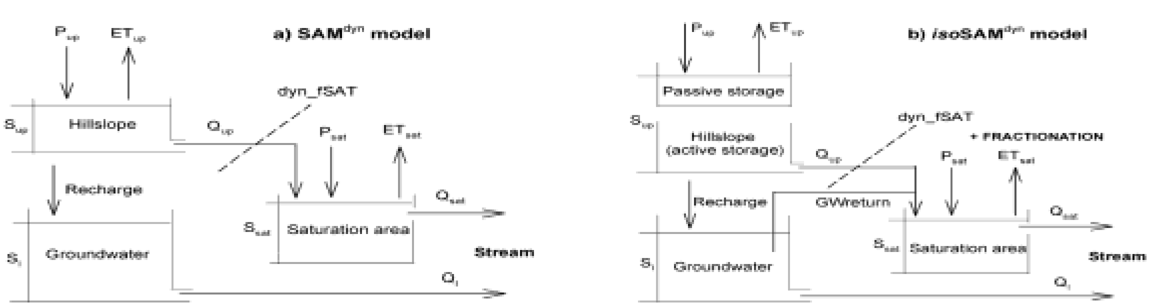

Figure 2. (a) Model concept of the original dynamic saturation area model (SAM^{dyn}) enabled to simulate isotope mixing and (b) the reconceptualized SAM^{dyn} model with additional passive storage, groundwater return flow, and fractionation processes (isoSAM^{dyn}).

$$Q_{up} = S_{up} k_1 ; \quad (4)$$

$$R = S_{up} r ; \quad (5)$$

$$Q_1 = S_1 k_2 ; \quad (6)$$

where k_1, k_2, r, and c (s^{-1}) are linear scaling parameters. The nonlinear saturation area storage (S_{sat}) is defined as

$$Q_{sat} = S_{sat}^{1+\beta} c ; \quad (7)$$

where β is a dimensionless nonlinearity parameter.

[16] To simulate the alkalinity concentration of the main water fluxes in the model, discharge-based functions were implemented into the saturation area and groundwater zones so that dynamic concentrations of Q_{sat} and Q_l could be derived. These were based on empirical measurements in the catchment as described by *Birkel et al.* [2010a]. The estimate alkalinity concentrations (μeq L^{-1}) for the saturation zone (Alk_{ns}) and groundwater runoff sources (Alk_{gw}) in the SAM^{dyn} model are

$$Alk_{ns} = 140 Q_{sat}^{-0.55} ; R^2 = 0.82 ; \quad (8)$$

$$Alk_{gw} = 750 e^{-1.2 Q_l} ; R^2 = 0.93 : \quad (9)$$

[17] For the present study, the SAM^{dyn} model was enhanced to incorporate isotope tracers directly linked to the water fluxes of the reservoir conceptualization. The isotope simulations are driven by daily precipitation and associated deuterium δ^2H signature equivalent to the difference of precipitation rate and evapotranspiration losses. This filters minor precipitation events from effectively reaching the hillslope and saturation zone storage. The model assumes instantaneous and complete mixing in the storage routine. This is represented by the total isotope tracer balance equation:

$$\frac{d(cS)}{dt} = A(c_P P - c\mathrm{ET}) - cQ ; \quad (10)$$

where S is total storage (m^3), ET is total evapotranspiration ($m\ s^{-1}$), c_P is the isotopic tracer composition (%) in total rainfall P ($m\ s^{-1}$) over the total catchment area (m^2), and c is the isotopic tracer composition (%) in the reservoir. Equation (10) allowed simulation of discharge and, most importantly, δ^2H as a time domain tracer, as well as alkalinity as a geographic source tracer.

[18] The simulated tracer stream signature δ^2HQ (%) is calculated via a weighted mean of saturation area and lower groundwater storage tracer (δ^2HQ_{sat}, δ^2HQ_l) and water (Q_{sat}, Q_l) flux:

$$\delta^2HQ = [(\delta^2HQ_{sat} Q_{sat}) + (\delta^2HQ_1 Q_1)]/Q : \quad (11)$$

[19] It should be noted that the simulated δ^2H values δ^2HQ_{up}, δ^2HQ_{sat}, and δ^2HQ_l can be compared to the measured signatures collected from the hillslope spring, the saturation zone, and the groundwater in wells, respectively. These comparisons provide a means for evaluating the internal isotope dynamics of the model as well as the outputs in streamflow. The time series were looped over 5 years for the model to warm up because of the relatively short study period. This facilitated the definition of the initial storage values and validation of the internal water balances.

Model Calibration and Evaluation

[20] For evaluation of the rainfall-runoff simulations, the Nash-Sutcliffe (NS) efficiency [*Nash and Sutcliffe*, 1970] and volumetric error (VE) criteria [*Criss and Winston*, 2008] were used as performance measures. For simulation of isotopes and alkalinity the coefficient of determination R^2 and the NS criterion were applied. The behavior of the model was evaluated using a stepwise, multicriteria calibration [*Khu et al.*, 2008] using tracer data in addition to discharge.

[21] 1. Monte Carlo (MC) random sampling with 100,000 iterations was used to assign parameter values to model simulations. Efficiency criteria for discharge and both tracers were evaluated for each iteration of the MC run.

[22] 2. On the basis of these results, efficiency criteria thresholds for discharge and tracers were subjectively established to maximum values for which it was still possible to identify acceptable parameter sets for all selected criteria. Model parameters were accepted as behavioral only when the following criteria were adhered to: (1) discharge Q with thresholds of $Q_{NS} > 0.6$ and $Q_{VE} > 0.75$, (2) stream alkalinity Alk with $Alk_{NS} > 0.6$, (3) stream deuterium δ^2HQ with NS > 0.2 and $R^2 > 0.4$, and (4) saturation area deuterium δ^2HQ_{sat} with $R^2 > 0.4$ (compared with the measured δ^2H in saturation area).

[23] 3. We attempt to reduce the subjectivity in the definition of behavioral parameter thresholds [*Stedinger et al.*, 2008] by taking additional δ^2H data which reflects information on the internal state of the system into the calibration procedure [*Winsemius et al.*, 2009]. The goal is to internally constrain the model to be consistent with measured data [e.g., *Seibert and McDonnell*, 2002 ; *Kirchner*, 2006]. Therefore, model runs were accepted as behavioral only when the following criteria were additionally adhered to: (1) an internal water balance error below 50 mm yr^{-1}, (2) simulated hillslope δ^2HQ_{up} of mean measured δ^2H in the

shallow spring plus or minus analytical error (0.63%), and (3) simulated groundwater 6^2HQ$_l$ of mean measured 6^2H in the deeper groundwater wells plus or minus analytical error(0.63%).

[24] 4. The 5th and 95th percentiles of simulated discharge, alkalinity, streamflow 6^2H, hillslope spring 6^2H, groundwater well 6^2H, and saturation area 6^2H at each time step, across all acceptable parameter sets, were used to define simulation envelopes representing uncertainty for flow and tracer simulation.

Parameter Identifiability

[25] Parameter identifiability was assessed to evaluate model hypotheses of catchment functioning and processes and whether parameter values were constrained by the data introduced additionally to discharge. The commonly used regional sensitivity analysis (RSA) was applied to evaluate how changes to model parameters might affect model predictions [*Hornberger and Spear*, 1981]. The uniformly sampled parameter space for initially unconstrained parameter ranges was compared against the parameter space

generated during model calibration using additional data to discharge. This procedure reflects the effect of constraints imposed on model parameters through data. The initial parameter space was sampled over a range from 0 to 1 for the five flow model parameters (k_1, k_2, r, c, and 2) and from 0 to 5000 for the isotope mixing parameter upS_d. The partitioning of the parameter space in behavioral and nonbehavioral simulations as suggested for RSA was performed according to the proposed multicriteria calibration (see section 4.2). The difference between the threshold criteria and each accepted performance measure was used to calculate a cumulative efficiency (cum Eff). The cumulative efficiency over the parameter ranges indicates parameter identifiability: A straight line indicates poor identifiability within the range and deviations indicate regions of identifiability. Higher gradients indicate clustering of behavioral simulations.

5. Tracer Hydrology of the Bruntland Burn

[26] Over the 13 month study period we observed slightly (~5%) drier conditions than the long-term average. The autumn and early winter of 2008 was a wet period, though late December was dry, and precipitation was greatest between January and February 2009 (Figure 3a). The greatest flow occurred in February in response to a rainfall event falling on a melting snow pack (Figure 3c). Drier conditions followed in spring (March – April), but the summer of 2009 was wet, preceding a dry September.

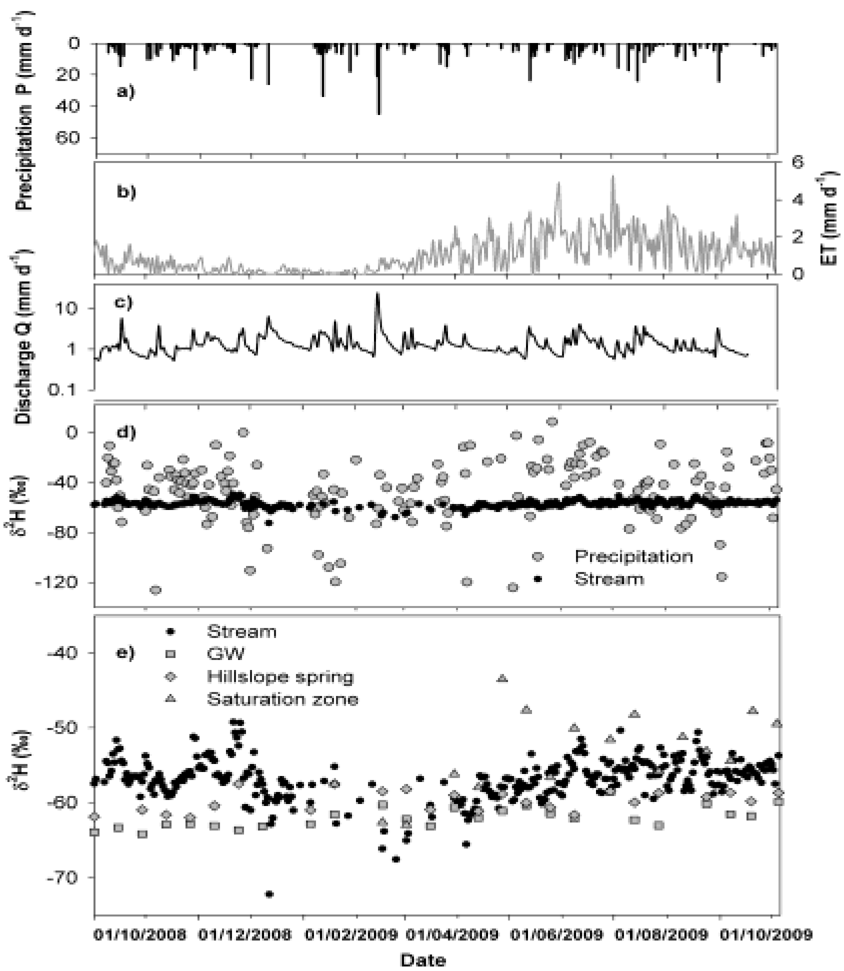

Figure 3. (a) Mean daily precipitation (P), (b) mean daily actual evapotranspiration (ET), (c) mean daily discharge (Q), (d) 6^2H deuterium signatures in daily precipitation and stream response (%), and (e) 6^2H deuterium signatures of streamflow, averaged groundwater wells (GW), hillslope spring, and averaged superficial saturation zone waters (%). Dates are given as day/month/year; read 1/10/2008 as 1 October 2008.

Flows were variable throughout the year, with high-flow events occurring each month. The evapotranspirationclosely followed the temperature regime, with greatest val- ues in summer (Figure 3b).

[27] Statistical summaries of the tracers in major water stores and fluxes are given in Table 2 ; however, it is the temporal dynamic of isotopic tracers that is most instruc- tive. The isotopic composition of daily precipitation varied throughout the year because of the relative uniformly dis- tributed wet Scottish climate, though the greatest fluxes of precipitation depleted in 6^2H occurred during the winter months and the greatest enriched fluxes occurred in summer (Figure 3d). Although greatly damped, stream iso- topes broadly reflect precipitation variation and seasonality (Figure 3d). That said, the greatest enriched stream 6^2H sig- natures were observed for a brief period in small events fol- lowing a warm, dry spell in November 2008 and more generally in summer 2009. Heavy winter storms cause a re-versal of in-stream 6^2H signatures to more negative values. Despite the coarser weekly sampling during this period the most depleted isotope characteristics are evident in events between December and February, including the snowmeltat the end of this period.

[28] Interestingly, even for flux-weighted averages, the mean 6^2H signature of stream water is not in equilibrium with the mean precipitation 6^2H signature (Table 2). This might be due to the relatively short 13 month sampling pe- riod with larger and more enriched summer precipitations than normal (Figures 3a and 3d). The averaged 6^2H signa- tures of groundwater samples are generally less than those of the stream, apart from periods following large winter events when surface waters are evidently depleted (Figure 3e and Table 2). This also implies aquifers being preferen- tially recharged by larger winter storms. In contrast, despite the shorter sampling period, the averaged saturation area samples generally show a more enriched 6^2H signature compared to streamflow and groundwaters, except during wet periods in the winter when the saturation of riparian zones is extensive (e.g., Figure 1) and significant propor- tions of the catchment are contributing directly to stream- flow [*Tetzlaff et al.*, 2007b]. This shows the importance of the saturation area not only for runoff generation but also as a mixing zone for new water entering the catchment as precipitation and old water already stored. It appears that the hillslope spring samples are slightly more enriched than those of deeper groundwater in the wells, implying the presence of shallower hillslope groundwater systems,which is consistent with the original model storage concept based on geochemical tracers and field observations [*Birkelet al.*, 2010a].

[29] Despite relatively few samples, the marked differ- ence between the saturation zone and groundwater compo- nents is apparent from the mean alkalinity values of 37 and 416 μeq L^{-1}, respectively (Table 2), and is consistent with earlier studies [*Soulsby et al.*, 2007]. We also find such dif- ferences in the 6^2H signatures of averaged saturation area waters and mean groundwaters (53% and 61%, respec- tively). The differences between the mean groundwater well (63%) and hillslope spring (60%) 6^2H signatures are more subtle, but compared to the analytical error for 6^2H, they are still significant. Both groundwaters show little tem-poral variability throughout the year (Table 2). Therefore, the definition of at least two distinct groundwater stores is consistent in both alkalinity and 6^2H measurements.

[30] Figure 4 shows the global meteoric water line (GMWL) regression compared to the daily precipitationsignatures, which lie reasonably close together and only slightly differ in their excess. On the basis of 6^2H and 6^{18}O measurements, a local evaporation line (LEL) regression was constructed (R^2 ¼ 0.98) for stream water and com- pared to the isotope compositions of groundwaters and sat- uration area waters. The stream water samples alone are located along a mixing line of water generated in colder and warmer periods. However, it is the location of the satu-ration zone samples and groundwater samples along the low gradient of the LEL (slope of 2.4) that indicate a con- tributing source to streamflow affected by isotopic fractio- nation processes. This is probably due mainly to evaporation, though snowmelt and even sublimation may also be important [*Lee et al.*, 2009]. Even though the ana- lytical error of isotope measurements has to be taken into account, the saturation area water samples plot on the right of the GMWL and along the LEL, whereas groundwater is located close to the GMWL and overlaps with streamflow,

Table 2. Summary Statistics of the Tracers Alkalinity and Deuterium (6^2H) in Stream Water, Precipitation (*P*), Snow, Groundwater Wells (GW) 1 and 2, Hillslope Spring (HS), and Saturation Zone[a]

Sample	Mean	Minimum	Maximum	Standard Deviation	90th Percentile	10th Percentile
6^2H (%)						
P (*n* ¼ 212)	–45.5	–167.2	1.8	27.4	–15.5	–73.3
Stream (*n* ¼ 318)	–56.6	–72.2	–49.2	2.7	–53.5	–59.6
Snow (*n* ¼ 8)	–104.2	–138.6	–69.1	24.4	–81.4	–131.3
GW well1 (*n* ¼ 31)	–62.5	–66.1	–59.9	1.6	–60.5	–64.9
GW well 2 (*n* ¼ 18)	–62.5	–66.3	–60.3	1.7	–60	–65
HS (*n* ¼ *28*)	–59.9	–62	–57.5	1.4	–58.3	–61.7
Saturation zone 1 (*n* ¼ 18)	–48.8	–65.4	–34.9	8.3	–37.8	–58.5
Saturation zone 2 (*n* ¼ 18)	–59.4	–63.8	–51.5	3	–57.1	–62.7
Saturation zone 3 (*n* ¼ 18)	–53	–63.2	–40.9	7.5	–44.1	–62.2
Alkalinity μ (meq L^{-1})						
Stream (*n* ¼ 47)	187.3	38.9	398	87.8	288.1	85
GW well 1 (*n* ¼ 4)	416	358	491	57.3	471	367
HS (*n* ¼ 3)	351	331	370	19.5	367	335
Saturation zone 3 (*n* ¼ 14)	36.8	—11.5	96.5	39.6	93.7	2.2

[a]Number *n* of samples is also given.

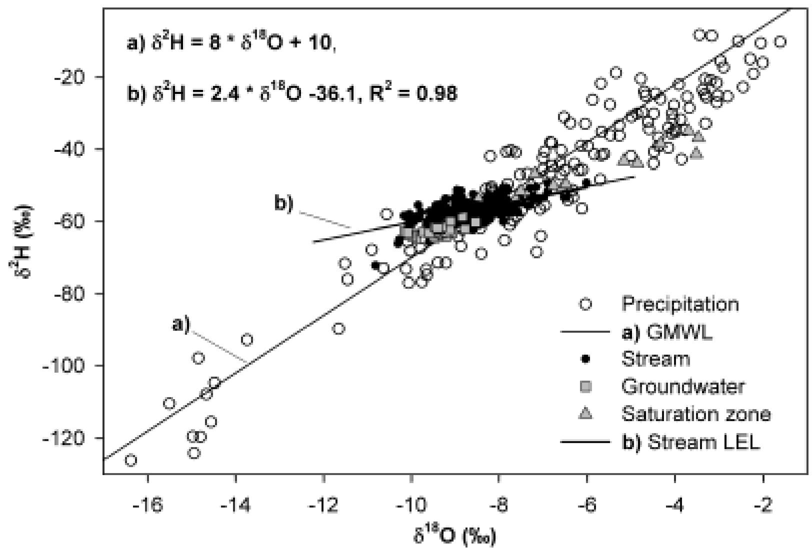

Figure 4. Precipitation isotopes, average groundwater, and average saturation zone waters plotted against the global meteoric water line (GMWL, line a) and the local evaporation line (LEL, line b) for stream water isotopes.

suggesting fractionation processes occur in surface waters of the saturated zone. Evaporative fractionation is most likely to be greatest in the perennial open water system of the saturation zone contributing directly to streamflow. However, no vapor isotope measurements are available to give clear evidence about significant or negligible fractionation due to evaporation and the effect on the streamflow isotope composition. The difference in isotopic signature between the stream, groundwater, and saturation zones further supports that saturation areas cannot simply be viewed as an expression of the groundwater table, but rather must be treated as distinct stores (especially during summer).

6. Incorporating New Insights From Time Domain Tracers Into isoSAM^{dyn}

[31] Figures 5a and 5b confirm the conclusions of earlier work by *Birkel et al.* [2010a], showing that for the study year, the basic SAM^{dyn} model could successfully simulate flows (range above threshold for discharge $0.6 < NS < 0.65$ and $0.75 < VE < 0.8$) and stream alkalinity (range above threshold for alkalinity $0.6 < NS < 0.64$) in the Bruntland Burn in a way that was consistent with field-based process understanding. The number of behavioral parameter sets could be constrained from 6208 accepted discharge simulations to 1054 using alkalinity additionally to discharge for calibration. The dynamics of the hydrograph are simulated reasonably well, capturing peak flows and recession periods (Figure 5a). The autumn and early winter (September – December 2008) low-flow period is less well reproduced than the summer 2009 period as low flows are generally overestimated, indicating that certain storage-runoff dynamics are not captured. With regard to stream alkalinity simulations, these also capture the general dynamics, though with a tendency to underestimate the alkalinity of low flows. This is a result of underpredicting the ground-water contribution to streamflow (Figure 5b). However, it might also indicate the errors involved in the parameteriza-

tion of alkalinity in the model and that only weekly samples were available. However, the soil water concentration of the quick flows below 100 μeq L^{-1} is simulated reason- ably well, especially in the case of the February 2009 win- ter storm. The source area contributions over the following 3 months, peaking at 400 μeq L^{-1}, are also well repre- sented (Figure 5b).

[32] However, as Figure 5c shows, attempts to simulate stream δ^2H with the original SAM^{dyn} model could not be accepted as behavioral. The variations in simulated isotope signatures are greatly exaggerated compared to those observed. This suggests the need to incorporate an addi- tional mixing volume (passive storage) into the model to account for the damping of the incoming precipitation sig- nal by increasing the residence time.

[33] In the revised model structure ($isoSAM^{dyn}$; Figure 2b) the hillslope storage is treated as unsaturated with a high passive (immobile) water content (passive storage in m^3) and mixing volume to facilitate isotope damping, as done by *Barnes and Bonell* [1996]. The groundwater and riparian storages are treated as saturated (active storage in m^3) with negligible passive water available [*Maloszewski et al.*, 1992]. This also results in only one additional param-eter. Because of the dynamic structure of the model, the mixing volume parameter passiveS_{up} was varied according to the estimated saturation area extent time series dyn_ fSAT, where greater saturation area extents result in a smaller hillslope storage area with potentially less passive water available for mixing:

$$\text{passive}\, S_{up} = V_{ini}(1 - \text{dyn\_fSAT}); \quad (12)$$

where V_{ini} is the calibrated initial mixing volume parameter (m^3) and dyn_fSAT volumetrically describes the saturation area and hillslope area extent (percent catchment area). The incorporation of passive storage into the water and mass balance of equation (1) calculates the total hillslope storage S_{up} as the sum of passive storage passiveS_{up} and active

International Journal of Engineering Sciences Paradigms and Researches (IJESPR)
Volume 46, Issue: Special Issue of December 2017
An Indexed, Referred and Peer Reviewed Journal with ISSN (Online): 2319-6564
www.ijesonline.com

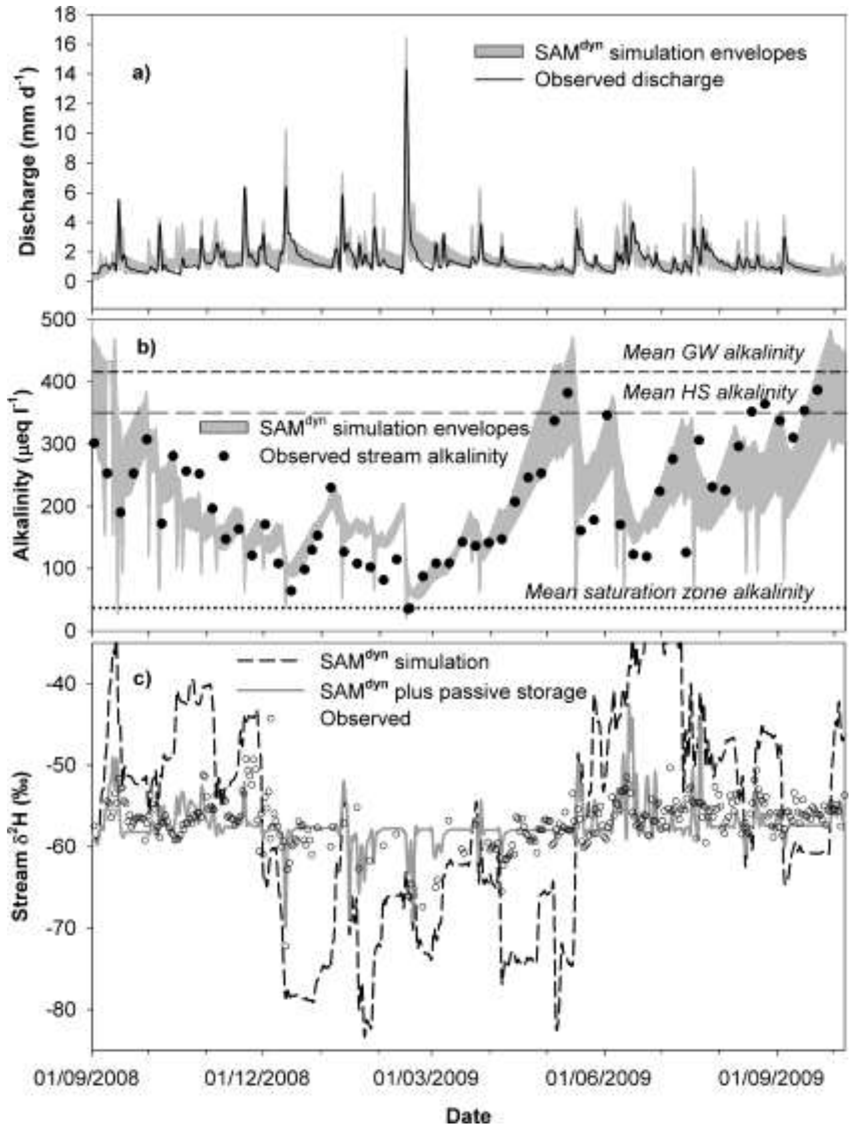

Figure 5. SAM^{dyn} (a) discharge and (b) stream alkalinity 5th and 95th percentile simulation envelopes applying the discharge and alkalinity calibrated model. The dotted line at 37 μeq L^{-1} and the dashed lines at 351 and 416 μeq L^{-1} indicate measured mean saturation zone, hillslope seepage (HS), and groundwater (GW) alkalinity concentrations, respectively. (c) Incorporation of isotope mixing into the dynamic saturation area model SAM^{dyn}. The simulation of stream 6^2H deuterium is demonstrated without further modifications to the original model concept (dashed line) and after an additional mixing volume in the hillslope storage (passive storage) was introduced (gray line) and applied with one accepted parameter set. Dates are given as day/month/year; read 01/09/2008 as 1 September 2008.

hillslope storage activeS_{up}. In this way, the water fluxes through the active storage are not altered by the passive storage. The active storage represents a state variable, and the passive storage represents a calibrated parameter. Incorporating this additional mixing volume into the hillslope storage water and mass balance of the isoSAM^{dyn} model improves the simulation of the overall stream isotope dynamics and event peaks substantially (Figure 5c). However, this still could not capture the fine detail of the observed daily isotope dynamics in the stream.

[34] A likely explanation for this is that waters of different sources mix in the saturation zone before reaching the stream. In the original version of SAM^{dyn}, the groundwater flow path was routed directly to the stream, bypassing the sat-

uration area zone without mixing (Figure 2a). While this was adequate for simulating alkalinity (Figure 5b), it seems inad- equate for simulating 6^2H (Figure 5c). To explore the impor- tance of the riparian area as a mixing zone, the model was modified to simulate the upwelling and mixing of ground- water in the saturation zone (Figure 2b). Consistent with field observations [*Soulsby et al.*, 1998], a groundwater flux

(GWreturn, m^3s^{-1}) was allowed to drain back into the ripar- ian area when the groundwater store is full, facilitating addi- tional mixing as well as Q_l discharging directly to the stream.

[35] In addition, the different waters plotted against the GMWL (Figure 4) indicated that fractionation due to evap- otranspiration and snowmelt was probably influencing iso- tope signatures, with the open water system of the riparian

International Journal of Engineering Sciences Paradigms and Researches (IJESPR)
Volume 46, Issue: Special Issue of December 2017
An Indexed, Referred and Peer Reviewed Journal with ISSN (Online): 2319-6564
www.ijesonline.com

saturation area being the most likely zone of influence. Therefore, the potential effect of fractionation in the saturation areas was also incorporated in the final isoSAM^{dyn} model using a kinetic fractionation algorithm in the riparian saturation zone mass balance. This allowed examination of the enrichment effect of evaporation on the daily deuterium signatures in the residual superficial waters prior to mixing with incoming water fluxes and reaching the stream. The isotopic signature of the loss term (evaporative flux) in the riparian storage mass balance was calculated with the *Craig and Gordon* [1965] model modified according to *Gibson and Edwards* [2002] to directly utilize isotopic data (in %),

$$\delta_E = \frac{\alpha \delta_{Sat} - h\delta_A - \varepsilon}{1 - h + 10^{-3}\varepsilon_K}; \qquad (13)$$

where α is the equilibrium liquid-vapor isotope fractionation, h is the atmospheric relative humidity normalized (from 0 to 1) to the saturation vapor pressure at the temperature of the air-water interface, and δ_A is the isotopic composition of ambient moisture.

[36] In the absence of direct measurements, we assume δ_A to be in equilibrium with the saturation area water, $\delta_A = \delta_{Sat}$[*Jouzel and Merlivat*, 1984], and

$$\varepsilon = \varepsilon_E + \varepsilon_K \qquad (14)$$

(in %), where the total isotopic separation factor $\varepsilon(\varepsilon = \alpha - 1)$ includes both equilibrium ε_E and kinetic ε_K components.

[37] The equilibrium fractionation coefficient can be estimated using empirical equations [*Araguas-Araguas et al.*, 2000]. The kinetic enrichment factor ε_E (%) depends on the boundary layer conditions and the humidity deficit h, estimated by

$$\varepsilon_K = C_K(1 - h); \qquad (15)$$

where experimentally determined C_K values of 12.5% for hydrogen are used to represent lake evaporation in the northern midlatitude hemisphere [*Araguas-Araguas et al.*, 2000]. The presence of saturation in the riparian zone throughout the year makes this a reasonable first approximation for this particular study catchment.

[38] A constant snowmelt fractionation was also introduced into the model when positive air temperatures were likely to generate melt. Because there were only 2 weeks of significant snowfall in the catchment in February, we did not incorporate a snowmelt routine in the model as maintaining low parameterization was a key objective. According to *Cooper* [1998], melt water from snow is an average of 15% depleted for deuterium (at equilibrium). This coefficient was directly added to hillslope and saturation zone fluxes in the water-isotope mass balance routine for inputs during the snow period from 18 February to 3 March 2009.

[39] Figure 6 shows the simulated δ^2H signatures in the saturation area before and after fractionation occurs and after mixing of upwelling groundwater. Unfortunately, the coarse, fortnightly sampling during this period misses much of the fine-scale variability, but the pattern of effective fractionation is consistent with the data. This indicated the observed snow period in winter (February– March) had depleted δ^2H signatures because of snowmelt fractionation, while evaporative fractionation in early spring (May) and summer (July– August) enriched the δ^2H signatures. There are also minor fractionation signals observable in spring and late summer. Thus, incorporation of fractionation and the mixing with upwelling groundwater apparently enabled isoSAM^{dyn} to better capture the observed isotope dynamics in the saturation areas. This can be seen in the simulated responses for April, mid-May, and July 2009. Highly positive precipitation inputs probably caused the overestimation of simulated δ^2H signatures in June 2009.

7. Reconciling the Temporal Isotope Dynamics With Conceptual Runoff Sources

[40] Parameter identifiability was assessed to evaluate whether additional data to discharge helped constrain model parameters and the model's degrees of freedom [*Fenicia*

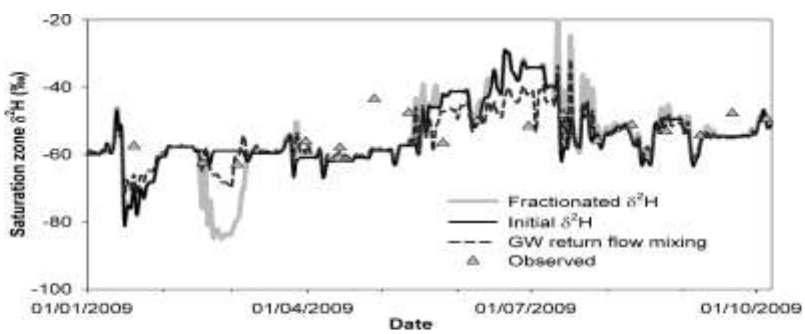

Figure 6. The effect of fractionation (snowmelt and evaporation) and mixing processes in the saturation zone (1 January to 7 October 2009) for the initial SAM^{dyn} plus passive storage simulation (black solid line) and for the simulation incorporating fractionation processes (gray line) and after mixing with groundwater (GW) return flow (dashed line) simulated with the new isoSAM^{dyn} model. Dates are given as day/month/year; read 01/01/2009 as 1 January 2009.

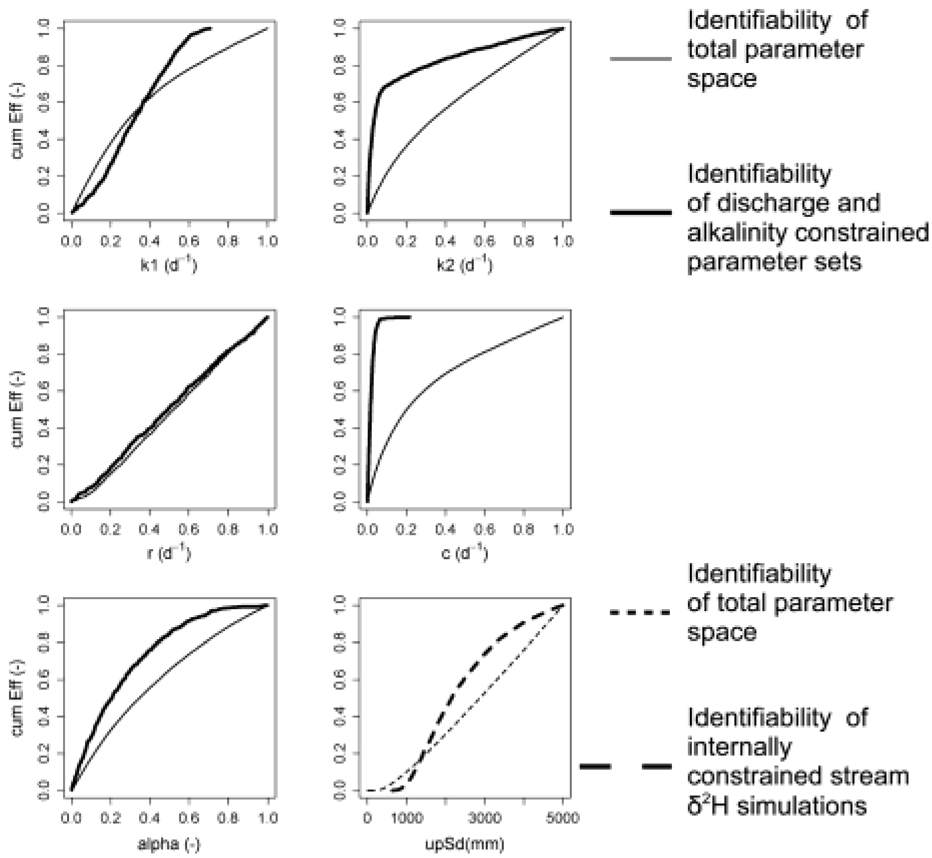

Figure 7. The cumulative efficiency (cum Eff) of model simulations is used to evaluate parameter identifiability for the unconstrained total parameter space, the discharge- and alkalinity-constrained simulations, stream 6^2H simulations, and the internally constrained stream 6^2H simulations.

et al., 2008]. Figure 7 indicates parameter identifiabilities expressed with cumulative efficiencies of the NS performance criteria for discharge, stream alkalinity, and stream 6^2H simulations, applying the reconceptualized isoSAM^{dyn} model. Figure 7 shows that the model parameters except for the recharge coefficient r and the isotope parameter upS_d are identifiable. However, multicriteria calibration of the model against discharge and alkalinity significantly constrained parameter ranges (k_1 and c) and increased identifiability (k_1, k_2, c, and 2). The recharge parameter r remained insensitive. Model calibration using internal state variables in the form of hillslope and groundwater 6^2H data also constrained the parameter range of upS_d and increased identifiability compared to the initial parameter space (Figure 7).

[41] The overall simulation of dynamics in streamflow 6^2H (range above threshold $0.2 < NS < 0.28$ and $0.4 < R^2 < 0.52$) are the best possible with the current model structure. The high-flow variations were generally captured, but daily variation in summer dynamics were particularly poorly represented (Figure 8b). The relatively constant isotopic compositions of the hillslope spring (Figure 8c) and groundwater (Figure 8d) were used to internally condition the model. These match mean signatures (Table 2) within analytical error intervals for the observed fortnightly 6^2H signatures of the hillslope spring and groundwater storages. The simulation of observed fortnightly saturation area signatures ranged above threshold $0.4 < R^2 < 0.48$, though

simulated values appear to underestimate the onset of fractionation processes in late April 2008 and to overestimate them during midsummer (Figure 8e).

[42] Simulation of the fine-scale 6^2H variability in daily streamflow remains problematic, especially during periods when fractionation caused by snowmelt or ET is important (Figure 8b). This is evident from the 2 week snow period at the end of February 2009 and during June and July in summer 2009. Inclusion of fractionation processes during these periods was needed to capture depleted signatures in winter and more enriched signatures in summer. However, this also leads to broader simulation bands for the saturation zone 6^2H (Figure 8e) and stream 6^2H (Figure 8b). This perhaps suggests overestimation of the evaporative fractionation effect and underestimation of the damping due to mixing processes taking place in the dynamic saturation areas before water reaches the stream (Figure 8b). Although, the 2 week snowmelt period partly consisted of a rain on snow event not captured by the simple fractionationcoefficient, the incorporation of snowmelt and evaporative fractionation improved the overall simulation of stream iso- tope signatures and is in line with observed data and pro- cess knowledge.

8. Discussion

[43] The hillslope – saturation area – groundwater model storage concept of the original SAM^{dyn} model was

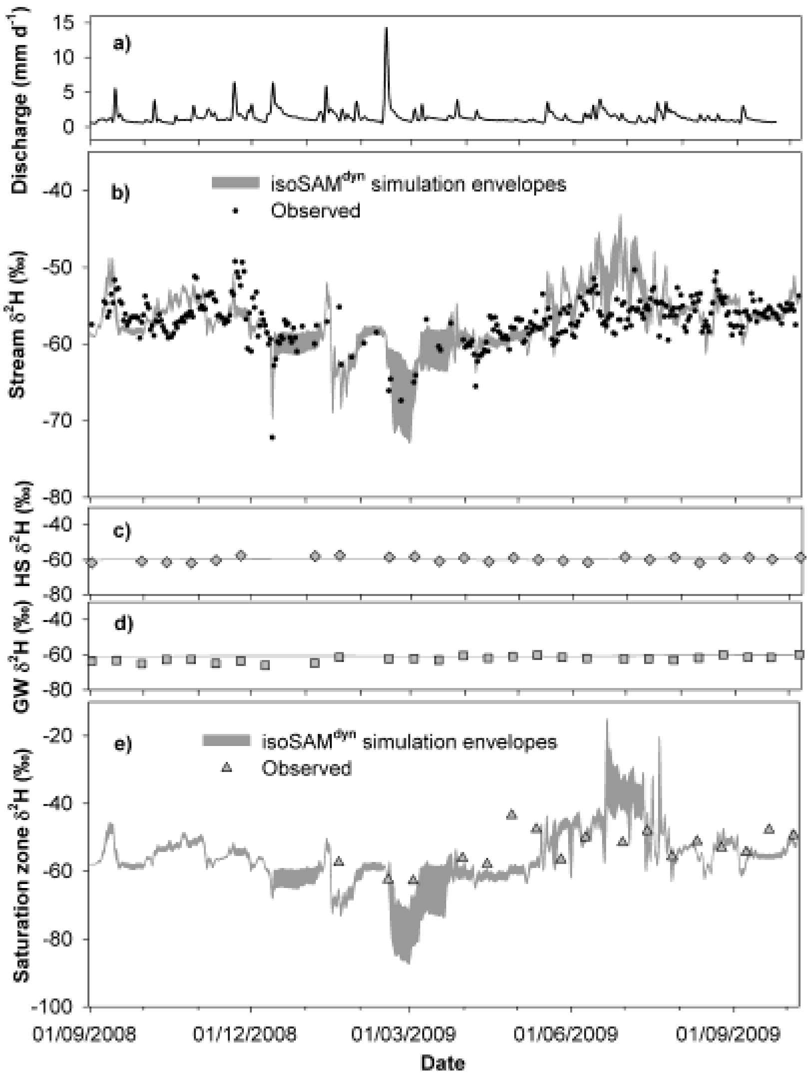

Figure 8. (a) Measured discharge and simulated δ^2H deuterium signatures in (b) stream water, (c) hill-slope spring (HS), (d) averaged groundwater (GW), and (e) averaged saturation area water for the study period 2008 – 2009, applying the multicriteria calibrated dual-tracer isoSAM^{dyn} model. The simulation envelopes indicate the 5th and 95th percentile prediction bounds. Dates are given as day/month/year; read 01/09/2008 as 1 September 2008.

developed following approaches similar to those of *Harris et al.* [1995], *Seibert et al.* [2003], and *Fenicia et al.* [2008]. This approach integrated field observations and tracer data for the BB catchment into a low-parameter (five) conceptual model that could simulate streamflows using the dominant geographic source areas of runoff in terms of groundwater contributions and the nonlinear generation of overland flow from dynamic saturation areas [*Birkel et al.*, 2010a]. However, the same model structure was unsuccessful in simulating the temporal variability of isotope dynamics in both stream waters and the main catchment source areas, which became apparent when using high-resolution precipitation and stream water samples. Most problematic was the inability of the original model to damp the incoming isotope signature. An additional storage parameter was needed in the new isoSAM^{dyn} model to facilitate sufficient mixing to damp the temporal variation in the deuterium signatures of precipitation inputs [*Fenicia* *et al.*, 2010]. In addition, the isotope data highlighted the importance of the riparian saturation areas as zones for run- off generation and solute mixing [*McGlynn and McDon- nell*, 2003 ; *Tetzlaff et al.*, 2008b; *Seibert et al.*, 2009].Thus, simulations were improved by routing some ground- water contributing to a mixing zone in the saturated area without changing the original source area conceptualization[*Anderson et al.*, 1997].

[44] Equally important to this improved representation of mixing processes was the recognition of the fractiona- tion process within the isotope dynamics. This was high- lighted by the change of slope of the stream LEL compared with the GMWL, representing the integrated effect of frac- tionation processes in the catchment due to evaporation in the saturation zones and snowmelt [*Gibson and Reid*, 2009 ; *Gibson and Edwards*, 2002 ; *Lee et al.*, 2009]. Inte- gration of fractionation processes generally improved the model simulations, and in the case of the snowmelt event,

fractionation was necessary to capture the depleted stream signatures. However, given the simplicity of the algorithm used [*O'Neil*, 1968 ; *Cooper*, 1998 ; *Luz et al.*, 2009], the uncertainty is high, and the study period is too short to esti- mate fractionation via an isotope mass balance [*He et al.*, 2003]. Even though the incorporation of fractionation proc-esses is in line with measured data and process understand- ing, more accurate means of quantification from direct measurement are needed to avoid the extrapolation of sparse and uncertain literature values. While this may increase the number of model parameters, the importance of fractionation processes in saturated zones may need to be more carefully considered in studies that are attempting to simulate isotopes in rainfall-runoff models. It is not nec- essarily the stream water itself that undergoes significant evaporation, but even in the relatively wet and cool Scot- tish climate, the saturation zones effectively act as open water systems throughout the year (comparable to shallow lakes) and alter the stream isotope composition by contrib- uting fractionated isotope content to the stream.

[45] The conceptualization of rainfall-runoff processes in the isoSAM^{dyn} model is broadly consistent with a field- based process understanding in the catchment [e.g., *Mal- colm et al.*, 2006 ; *Soulsby et al.*, 2007 ; *Tetzlaff et al.*,2007b]. As shown in other studies in the Scottish Highlands[e.g., *Soulsby et al.*, 1998, 2000], deeper groundwaters (of- ten with a bedrock influence) are isotopically and geo-chemically distinct from spring seepage of shallower groundwater systems (in hillslope colluvium) which drain directly into the riparian zones (Figure 2b and Table 2). However, the dynamics of riparian saturation zones are key to understanding the hydrology and tracer dynamics of this catchment. The dual-tracer approach has shown that the model simulates observed tracer signatures of the dynamics of different source components reasonably well. This better reflects catchment behavior than only using geographic source area tracers as in SAM^{dyn} and thus justifies the use of isotopic tracers as additional data in model assessment [*Seibert and McDonnell*, 2002]. The use of soft data con- strained model parameters and improved parameter identi- fiability (Figure 7), which, most importantly, conditioned the model toward simulations consistent with process knowledge. Furthermore, the use of isotope data of catch- ment stores constrained the tracer mixing parameter. This might allow, in turn, more accurate estimations of catch- ment storage volumes [*Kirchner*, 2006]. The inferred pas- sive storage (broadly identifiable between 2700 and 4200 mm, Figure 7) needed to damp tracer concentrations in the model is an order of magnitude greater than the dynamic storage variations as a result of seasonal variations of water balance components. While these figures should be viewed as indicative rather than definitive, such passive storage has been shown in experimental studies [*Engler et al.*, 2008], and they are of the same order of magnitude as those inferredby lumped parameter transit time modeling of the BruntlandBurn using independent data [*Soulsby et al.*, 2009].

[46] This study, for the first time, used both daily 6^2H and 6^{18}O water stable isotopes collected over more than a hydrological year to explore rainfall-runoff processes in a Scottish upland catchment, applying an iterative model approach testing different hypotheses of runoff generation mechanisms. This unique data set is consistent with previ-

ous process conceptualizations based on geographic source tracers and field studies in the area but emphasizes the need to consider and further develop the passive storage concept in catchments, the role of riparian saturation zones laterally and vertically redistributing water and solutes to the stream, and the role of isotopic fractionation processes due to snowmelt and evaporation. Fractionation has rarely been incorporated in catchment isotope-based process models because of data constraints. Hence, the daily isotope record refined the understanding of temporal rainfall-runoff dy- namics compared to a coarser (e.g., weekly) sampling reso-lution [*Birkel et al.*, 2010b].

[47] Even though much work remains on testing the underlying assumptions of solute mixing [*McGuire et al.*, 2006 ; *Fenicia et al.*, 2010], a novel element of this study included the examination of the isotope dynamics of inter- nal catchment stores, rather than just the rainfall-runoffrelationship [*Bowden et al.*, 2001 ; *Seibert et al.*, 2009]. Such measured data of internal catchment states could be used more rigorously in the future to avoid subjectivity in model calibration procedures [*Winsemius et al.*, 2009]. There is also potential for more sensitive model evaluation, especially when a better process representation consistent with data does not necessarily improve statistical perform- ance measures [*Fenicia et al.*, 2010].

References

Anderson, S. P., W. E. Dietrich, D. R. Montgomery, R. Torres, M. E. Con- rad, and K. Loague (1997), Subsurface flow paths in a steep, unchanneled catchment, *Water Resour. Res.*, *33*, 2637–2653.

Araguas-Araguas, L., K. Froehlich, and K. Rozanski (2000), Deuterium and oxygen-18 isotope composition of precipitation and atmospheric moisture, *Hydrol. Processes*, *14*, 1341–1355.

Barnes, C. J., and M. Bonell (1996), Application of unit hydrograph techni-ques to solute transport in catchments, *Hydrol. Processes*, *10*, 793–802.

Berman, E. S. F., M. Gupta, C. Gabrielli, T. Garland, and J. J. McDonnell (2009), High-frequency field-deployable isotope analyzer for hydrologi- cal applications, *Water Resour. Res.*, *45*, W10201, doi:10.1029/ 2009WR008265.

Beven, K. (2007), Towards integrated environmental models of every- where: Uncertainty, data and modelling as a learning process, *Hydrol. Earth Syst. Sci.*, *11*, 460–467.

Birkel, C., D. Tetzlaff, S. M. Dunn, and C. Soulsby (2010a), Towards sim- ple dynamic process conceptualization in rainfall-runoff models using multi-criteria calibration and tracers in temperate, upland catchments, *Hydrol. Processes*, *24*, 260–275.

Birkel, C., S. M. Dunn, D. Tetzlaff, and C. Soulsby (2010b), Assessing the value of high-resolution isotope tracer data in the step-wise development of a lumped conceptual rainfall-runoff model, *Hydrol. Processes*, *24*, 2335–2348.

Bowden, W. B., B. D. Fahey, J. Ekanayake, and D. L. Murray (2001), Hill- slope and wetland hydrodynamics in a tussock grassland, Southland, New Zealand, *Hydrol. Processes*, *15*, 1707–1730.

Cooper, L. W. (1998), *Isotopic fractionation in snow cover, in Isotope Tracers in Catchment Hydrology*, edited by C. Kendall and J. J. McDon-nell, pp. 119–136, Elsevier, Amsterdam.